Published in final edited form as:
Cancer Prev Res (Phila). 2011 November ; 4(11): 1884–1894. doi:10.1158/1940-6207.CAPR-11-0221.

Phenylbutyl Isoselenocyanate Modulates Phase I and II Enzymes and Inhibits 4-(Methylnitrosamino)-1-(3-pyridyl)-1-butanone Induced DNA Adducts in Mice

Melissa A. Crampsie[1], **Nathan Jones**[1], **Arunangshu Das**[3,4], **Cesar Aliaga**[3,4], **Dhimant Desai**[1,4], **Philip Lazarus**[2,4], **Shantu Amin**[1,4], and **Arun K. Sharma**[1,4,*]

[1]Department of Pharmacology, Penn State Hershey College of Medicine, 500 University Drive, Hershey, PA 17033.

[2]Department of Public Health Sciences, Penn State Hershey College of Medicine, 500 University Drive, Hershey, PA 17033.

[3]Department of Biochemistry and Molecular Biology, Penn State Hershey College of Medicine, 500 University Drive, Hershey, PA 17033.

[4]Penn State Hershey Cancer Institute; Penn State Hershey College of Medicine, 500 University Drive, Hershey, PA 17033.

Abstract

Lung cancer remains one of the most preventable forms of cancer with about 90% of cases attributed to cigarette smoking. Over the years, the development of chemopreventive agents that could inhibit, delay, or reverse the lung carcinogenesis process has been an active field of research, however, without much attainment. Through extensive structure-activity relationship studies, we recently identified a novel agent phenylbutyl isoselenocyanate (ISC-4), designed based on naturally occurring isothiocyanates well known for their lung cancer prevention properties, as a potential chemopreventive agent. In the present study, we used A/J mice to evaluate the lung cancer chemopreventive potential of ISC-4. A single intragastric dose of 1.25 μmol ISC-4 resulted in a time-dependent increase of selenium levels in serum, liver, and lung, suggesting that ISC-4 is orally bioavailable, a key requirement for a chemopreventive agent. This dose also resulted in a time dependent inhibition of microsomal cytochrome P450 (Cyp) activity and delayed increases in Phase II UDP-glucuronyl transferase (Ugt) and glutathione-S-transferase (Gst) activity. ISC-4 was able to induce mRNA expression of Cyp, Ugt, and Gst enzyme isoforms in liver, but in lung inhibited Cyp isoforms while inducing Ugt and Gst isoforms. In addition, ISC-4 effectively inhibited methyl-DNA adduct formation in mice fed diet supplemented with ISC-4 for two weeks and then treated with the tobacco procarcinogen 4-(methylnitrosamino)-1-(3-pyridyl)-1-butanone (NNK). These results suggest that ISC-4 is a strong candidate for development as a chemopreventive agent.

[*]*Author to whom correspondence should be addressed*, Arun K. Sharma, Ph.D., Penn State Milton S. Hershey Medical Center, Penn State College of Medicine, Department of Pharmacology, Penn State Hershey Cancer Institute, CH72, 500 University Drive, Hershey, PA 17033, Phone: 717-531-0003 ext. 285016, Fax: 717-531-0244, aks14@psu.edu.

Disclosure of Potential Conflicts of Interest
No potential conflicts of interest were disclosed

Introduction

Lung cancer is the leading cause of cancer death worldwide with a 5 year survival rate of only 15% (1). It is also one of the most preventable forms of cancer due to the fact that 90% of cases are attributed to smoking and/or chewing tobacco, thus the majority of prevention efforts are focused on smoking cessation. For those who cannot quit due to the addictive nature of nicotine, and for former smokers who may be at high risk for developing lung cancer, chemoprevention strategies may be the answer. Lung cancer development in smokers and former smokers can have a latency period of 10–30 years (2), allowing for a significant time frame to intervene in the carcinogenesis process. Therefore, cancer chemoprevention, which seeks to arrest or reverse the disease process of carcinogenesis in its initiation, promotion and progression toward invasive malignancy, holds a great scientific promise. However, optimal prevention of lung cancer has not been achieved yet due to the lack of an effective and safe chemopreventive agent.

Epidemiological studies have provided evidence that consumption of cruciferous vegetables, such as broccoli and cauliflower, is associated with a decreased risk of developing several types of cancer at a variety of organ sites (3–5). The effect is attributed to a class of chemicals known as isothiocyanates (ITCs) that are stored in cruciferous vegetables as their glucosinolate precursors (6–8). There is strong literature data demonstrating ITCs to be effective chemopreventive agents for specific human cancers (3, 9–13). ITCs have been shown to exhibit their anticarcinogenic effects through dual mechanisms occurring at the level of initiation of carcinogenesis by blocking Phase I enzymes (cytochrome P450) that activate procarcinogens and also by inducing Phase II enzymes that detoxify electrophilic metabolites generated by Phase I enzymes (14–16). Specifically, they have been shown to be very effective in modulating tobacco carcinogen 4-(methylnitrosamino)-1-(3-pyridyl)-1-butanone (NNK) metabolism and are potent inhibitors against NNK-induced lung tumorigenesis in A/J mice (17, 18). NNK requires metabolic activation by cytochrome P450 to exhibit its mutagenicity and possible carcinogencity (19) (Figure 1). Hydroxylation of the alpha carbons yields two reactive species, which alkylate DNA to produce pyridyloxobutyl (pob)-DNA or methyl-DNA adducts. This is believed to be an important mechanism of carcinogenesis in both rodents (20–22) and smokers (23, 24), since pob-DNA adducts have been detected in animals treated with NNK and in the lung tissue from smokers (24). Furthermore, the O^6-methyl guanine (O^6-MG) adducts have been determined to be critical for tumor formation in A/J mice treated with NNK and is less efficiently repaired in the presence of bulky pob-DNA adducts (25, 26). The chemopreventive efficacy, favorable mechanism of action, and safety profile of ITCs in general and towards NNK induced carcinogenesis in particular, makes them ideal lead compounds for structural optimization.

Our lab has modified both naturally occurring and synthetic phenyl alkyl ITCs by isosterically replacing sulfur with selenium to make isoselenocyanate (ISC) compounds (27). The rationale for this modification was based on the observation that organoselenium compounds have been shown to be effective in retarding tumorigenesis of several cancer types (28–31), in both animal models and epidemiological studies. Hence, ISC compounds combined the anticancer properties of both selenium and ITCs. Furthermore, compared to sulfur structural analogs, selenium compounds have been shown to be more potent anti-cancer agents (32). We have also found the selenium compounds (ISCs) to be more potent in cell viability and animal bioassays for cancer as compared to the corresponding ITC derivatives (27). Extensive structure-activity studies on ITCs and newly generated ISCs have identified phenylbutyl isoselenocyanate (ISC-4) (Fig. 2A) as the most efficacious agent both in terms of potency and drug-likeness (27, 33).

The suitability of ISC-4 as a chemopreventive agent was tested in an animal model of lung cancer using A/J mice. These mice are susceptible to Ki-ras mutations which lead to 20–40% of them to spontaneously develop lung adenomas by 20 weeks of age (34). Treatment with NNK leads to DNA adducts and 100% incidence of lung tumors in these mice only 16 weeks after carcinogen administration, regardless of the route of administration (34). To assess the chemopreventive potential of ISC-4, intragastric dosing of the drug was first established and then mice were analyzed for Phase I and II enzyme activity and gene expression after a single dose of the drug in a time dependent manner. Mice were also treated with the procarcinogen NNK to determine if ISC-4 was able to inhibit DNA adduct formation in liver and lung.

Materials and Methods

Chemical and reagents

ISC-4 was synthesized following a method recently developed by Sharma *et al.* (27). ^{3}H[NNK] was purchased from Moravek Biochemicals (Brea, CA). The deuterated pob adduct standards were a kind gift from Dr. Stephen Hecht (University of Minnesota Cancer Center, Minneapolis, MN). Glucose-6-phosphate (G-6-P), $NADP^{+}$, G-6-P dehydrogenase, phosphodiesterase II, alkaline phosphatase, guanine, O^{6}-methyl guanine (O^{6}-MG), and 7-methylguanine (7-MG) were purchased from Sigma Aldrich (Milwaukee, WI).

Animal experiments

Animal experimentation was carried out according to protocols approved by the Institutional Animal Care and Use Committee (IACUC) at Penn State University. Female A/J mice were purchased at 6 weeks of age from The Jackson Laboratory (Bar Harbor, ME) and stratified into groups by treatment of ISC-4. Mice were given corn oil (vehicle control) or ISC-4 dissolved in corn oil at 2.5 ppm, 5.0 ppm, or 10.0 ppm (as selenium) per mouse (20 g average). Mice were sacrificed by CO_2 asphyxiation, organs harvested and immediately frozen on dry ice. Serum was collected from blood immediately by centrifugation. Tissue and serum samples were stored at −80 °C until analysis.

Selenium analysis

Liver or lung tissue (0.100 g to 0.400 g) was homogenized in 1.15% cold KCl (0.1 gm/ml) using a glass hand homogenizer. Exact amount of tissue homogenate or 200 µl serum was digested in a MARS Xpress microwave digestion system (CEM Corp., Mathews, NC) equipped with 55 ml Teflon PFA vessels and a turntable. The digestion was conducted in 50% nitric acid and was diluated to 20% before Se analysis by Atomic Absorption Spectroscopy. An AAnalyst 600 instrument from PerkinElmer with Graphite Furnace was used for total selenium analysis by measuring the absorbance peak area at 196 nm for each sample. Palladium matrix modifier was added along with each sample to the furnace. A reference standard solution of selenium dioxide was used to construct standard curve. Analysis was performed in duplicate for each sample and the average value was recorded. For each group or category at least three samples were analyzed and the results were expressed as mean ± SD (n=3).

Microsome and cytosol fraction preparation

Liver and lung microsomes or cytosol extracts were prepared as previously described (35). Briefly, homogenate was centrifuged once at 10000×g to remove nuclear pellet, then at 105000×g for cytosol extract (supernatant). The remaining pellet was resuspended and spun at 105,000×g for microsomes (pellet). Fractions were stored at −80 °C until use. Protein

concentrations for microsomes and cytosol fractions were determined using a BCA protein assay kit (Pierce, Rockford, IL).

Cyp activity assay with the substrate NNK

Microsomal Cyp activity was assayed in 150 µl 0.1 M Tris (pH 7.4), 1 mM EDTA, 20 mM $MgCl_2$, and 0.3 M KCl. Cyp activity was induced by an NADPH generating system (1 µg/µl G-6-P and $NADP^+$, 0.4 mU/µl G-6-P dehydrogenase). ^{3}H[NNK] was added at 0.5 µCi/reaction. Non-radiolabeled NNK was added to 20 µM. Reactions were initiated by addition of microsomes (1 mg/ml) and incubated at 37 °C for 1 h. Reactions were terminated with cold 7.5 M NH_4Ac, vortexed, and placed on ice for 10 min. Tubes were centrifuged for 10 min at 14000 rpm. Samples were filtered and analyzed by HPLC (Waters, Milford, MA) for oxidative metabolism of NNK using Radio Flow Detection (INUS Systems). A Phenomenex Max-RP C18 reverse phase column was used to separate metabolites. The HPLC conditions were 100% solvent A (25 mM sodium phosphate, pH 7.0)/0% B (Methanol) to 70% A/30% B with a linear gradient over 50 min. Cyp activity was calculated based on mean peak areas of metabolites formed in triplicate reactions.

Ugt activity assay with the substrate 4-methylumbelliferone (4-MU)

Mouse liver microsomes (10 µg protein) were assayed for Ugt activity in 100 µl reaction buffer (50 mM Tris pH 7.5, 10 mM $MgCl_2$, 10 µg/ml alamethicin, 4 mM UDPGA) using 4-MU as the substrate at 100 µM (liver) or 250 µM (lung). Reactions were initiated by addition of microsomes and incubated at 37 °C for 15 min. Reactions were terminated with 100 µl cold acetonitrile. Tubes were centrifuged for 10 min at 14000 rpm. Samples were filtered and analyzed by HPLC (Waters) for glucuronidation of 4-MU. Glucuronide and parent compound were eluted isocratically at a flow rate of 1 ml/min with 80% A (3.5% triethylamine, pH 2.1 with perchloric acid)/20% B (acetonitrile) v/v using a Phenomenex Max-RP C18 reverse phase column and measuring fluorescence (365 nm/455 nm) and UV at 318 nm. Glucuronidation activity was determined by the ratio of the 4-MU glucuronide peak compared to the unconjugated 4-MU peak.

Ugt activity assay with the substrate 4-(methylnitrosamino)-1-(3-pyridyl)-1-butanol (NNAL)

Mouse liver microsomes (50 µg protein) were incubated with alamethicin (10 µg/ml) on ice for 15 minutes. 25 µl reactions containing 5 mM NNAL were incubated at 37 °C for 1 h using the same conditions as for 4-MU. NNAL glucuronidation activity assays were analyzed using an Acquity UPLC system (Waters) with an ACQUITY UPLC BEH HILIC (2.1 mm × 100 mm, 1.7 µm particle size; Waters) column at 25 °C. UPLC was performed at a flow rate of 0.5 mL/min using the following conditions: 6.0 minutes in 10% solvent A, a linear gradient for 1.5 minutes to 100% solvent A, and 30 seconds in 100% solvent A, where solvent A is 5 mM NH_4Ac (pH 6.7) and 50% acetonitrile (v/v) and solvent B is 5 mM NH_4Ac (pH 6.7) and 90% acetonitrile (v/v). UV absorbance at 254 nm was used to detect NNAL and NNAL glucuronide. The amount of NNAL glucuronide formed was calculated based on the ratio of the NNAL-glucuronide peak compared to the unconjugated NNAL peak.

Gst activity assay

Cytosolic Gst activity was assayed by diluting cytosol extracts to 1 mg/ml with Dulbecco's PBS and measuring the rate of GSH conjugation with monochlorobimane (MCB) (excitation/emission: 380 nm/460 nm). 10 µl of 10 mM GSH was added to 100 µl of cytosol in 96 well black wall plates. 100 µl of 0.3 mM MCB was added to start reaction. The reactions (n = 3) were kinetically monitored by Spectromax spectrophotometer at 37 °C until a fluorescence plateau. All samples were measured in triplicate. Gst conjugation rates

were determined by measuring the time for all the GSH to be conjugated to MCB and finding the v50 using the Boltzman equation (Graphpad 5.0).

RNA extraction and cDNA synthesis

Total RNA was extracted from liver and lung tissue samples using RNeasy Mini Kit (Qiagen) according to manufacturer's protocol. Samples were subjected to on-column DNAse I digestion during extraction to prevent confounding of the results by genomic DNA contamination. RNA concentrations were determined using a Nanodrop ND-1000 spectrophotometer, and RNA purity was assessed by absorbance ratios A260/A280 (> 1.9). RNA integrity was determined using an Agilent 2100 Bioanalyzer with Agilent RNA 6000 Nano chips. RNA integrity of all samples was greater than 5.0. Reverse transcription was performed using Superscript First Strand cDNA synthesis kit (Invitrogen) with 1 μg of starting RNA per sample. A negative control without RNA and a negative control without enzyme were analyzed in parallel.

Relative expression levels of Cyp, Ugt, and Gst genes using real time qPCR

Real-time PCR was used to determine the relative expression levels of Cyps (2a4, 2c29, 2f2, 2s1, 3a11, 4b1, and 8b1), Gsts (Gsta3, Gsta4, Gstm1, Gstm2, Gstm3, and Gstp1), and Ugts (1a1, 1a5, 1a6a, 1a9, 1a10, 2a3, 2b1, and 2b5) in liver and lung tissue using Taqman gene expression assays (Applied Biosystems) utilizing predesigned primers. cDNAs were run in quadruplicate and amplified in a 10 μl reaction containing 5 μl 2× Taqman Universal PCR Master Mix, 0.5 ml 20× primer/probe mix, and a 25ng RNA equivalent of cDNA. Relative quantification of expression was calculated using the ΔΔCt method. Relative quantification (RQ) was determined with the formula $2^{(-\Delta\Delta Ct)}$. Expression levels in each sample were normalized to three separate internal control genes (ACTB, HPRT, and TBP), and final RQ values were calculated by taking the geometric mean of the individual RQ values. Several studies have shown that normalization to multiple internal control genes reduces systematic error and allows small changes in gene expression to be detected more accurately(36–42).

DNA adduct analysis

For DNA adduct studies, mice were fed control diet (AIN-76A) or diet supplemented with 0.57 μmol/g diet ISC-4 for two weeks. Mice were then given a single intraperitoneal (IP) dose of 10 μmol NNK in saline and sacrificed either 4 h (methyl adducts) or 24 h (pob adducts) after NNK. DNA was extracted from lung or liver tissues by phenol-chloroform extraction method and dissolved in TE buffer. DNA was quantified by a Nanodrop ND-1000 spectrophotometer. For pyridyloxobutyl (pob) adducts, 100 μg of DNA in calcium chloride buffer was hydrolyzed with deuterated standards for 30 min at 90 °C and then enzymatically digested to nucleosides with micrococcal nuclease, phosphodiesterase II, and alkaline phosphatase at 37 °C overnight. The samples were then purified on Sep Pak C18 cartridges (Phenomenex) and analyzed by HPLC-Mass Spectrometry. Samples were normalized first by internal deuterated standards and then by total nucleoside content. For methyl adduct analysis, 200 μg – 300 μg of DNA was hydrolyzed in 0.1 N HCl for 30 min at 100 °C. Samples were filtered and analyzed by HPLC on a strong cation exchange column (Phenomenex) using UV and fluorescence detection (Waters). Adducts were eluted isocratically with 100 mM ammonium phosphate buffer, pH 2.0. Peaks were quantified using guanine, 7-MG, and O^6-MG standard curves.

Data analysis and statistics

Statistical analyses were done using GraphPad Prism version 5.0. Mean values for activity assays or gene expression were compared across the treatment or time groups using 1-way analysis of variance (ANOVA) with significant p-value < 0.05. A student's t-test was used

to compare individual treatment groups or time point groups to the control group when ANOVA values approached but did not reach significance (ANOVA *p*-value 0.05–0.10).

Results

ISC-4 is orally bioavailable in A/J mice

ISC-4 was given to A/J mice intragastrically to determine its oral bioavailability by measuring selenium levels in serum and target organs. To determine an effective and tolerable dose, ISC-4 was administered to animals at increasing doses of 0.675, 1.25, and 2.5 μmol per mouse (n = 6 per group). At 2.5 μmol (30 mg/kg), half of the mice died within 24 h, so no doses higher than this were tested. At 1.25 μmol (15 mg/kg) and 0.675 μmol (7.5 mg/kg) mice appeared as healthy as the corn oil treated control mice. Three mice from each group were analyzed for selenium content after 24 h. Liver and serum from each mouse was analyzed separately, but lungs were pooled. Selenium content in serum, lung, and liver increased in a dose dependent manner (Figure 2B). This indicated that selenium content from ISC-4 was being absorbed into the blood and reaching target tissues. For a complete time course study, mice (n=3) were dosed with 1.25 μmol ISC-4 and sacrificed at 0, 2, 4, 8, 16, 24, 36, and 72 h (Figure 2C). The time course study showed that selenium levels peaked first in serum (max. mean 1892 ng/g) at about 4 h post ISC-4 administration, followed by liver between 4–8 h (max. mean 1322 ng/g) and lung at about 8 h (max. 878 ng/g) post administration. Selenium levels began to fall to near normal levels between 24–72 h but did remain slightly elevated when compared to the zero time point even up to 72 h. (serum $p = 0.058$, liver $p = 0.0072$).

Cytochrome P450 activity is decreased in liver and lung of mice treated with ISC-4

Cyp450 activity was analyzed by incubating liver or lung microsomes from mice (n=3) at each time point with ^{3}H[NNK] and measuring the metabolic profile (Figure 3A, 3B) by HPLC. Our results indicate that Cyp450 activity is decreased after oral administration of ISC-4 in both the liver and lung as evidenced by the decreased levels of keto acid, keto alcohol, and NNK-N-oxide (lung only) metabolites formed. Inhibition of metabolites occurred almost immediately after administration of ISC-4 (as early as 0.5 h in liver) and metabolites remained inhibited up to 24 h in liver and up to 12 h in lung. Inhibition of Cyp enzymes lasted longer in the liver which correlates with the higher selenium levels seen in the liver as compared to the lung (Figure 1C). Our results also indicate that conversion of NNK to NNAL, a detoxification pathway facilitated by a carbonyl reductase, remains unchanged or slightly elevated at each time point. To determine the concentration of ISC-4 required for microsomal Cyp450 inhibition, control liver microsomes were incubated with ISC-4 in DMSO at a range of doses and formation of NNK metabolites were measured. Inhibition of Cyp450 oxidative metabolism began as low as 25 nM ISC-4 and was dose dependent (Figure 3C, 3D).

Ugt activity against 4-MU and NNAL

In humans, NNAL is *N*-glucuronidated primarily by the hepatic UGT2B10 and *O*-glucuronidated by UGTs 1A9, 1A10, 2B7 and 2B17 (43, 44). Real-time PCR assays were performed for the mouse ortholog of 2B10, Ugt2b34 (see Table 1) and it was found to be expressed in mouse liver but not lung (results not shown). NNAL glucuronidation was measured using liver microsomes (Figure 4A), but NNAL glucuronidation activity could not be detected with mouse lung microsomes. Therefore the substrate 4-MU, which is glucuronidated by all human UGT1A enzymes as well as UGT2B enzymes except 2B4 and 2B10 (45), was used as a test substrate to determine overall glucuronidation activity of mouse lung and liver microsomes (Figure 4B, 4C). For liver microsomes, glucuronidation activity was increased after 8 h for NNAL ($p<0.0001$), but not for 4-MU where

glucuronidation activity appeared to decrease, though not significantly (One way ANOVA = 0.09). For lung microsomes, 4-MU glucuronidation was significantly increased at 24 h (p=0.0016) post ISC-4 administration.

Gst activity against monochlorobimane

Cytosolic fractions were incubated with monochlorobimane (MCB), a nonspecific substrate conjugated by all human GST isoforms except GSTT (46) (mouse ortholog Gstt see Table 1), to assess Gst activity. Liver cytosol activity against MCB was 20–50 fold higher than in lung (Figure 4D, 4E). In liver, Gst activity was significantly increased at 16 h post ISC-4 administration (p=0.049) and 24 h post ISC-4 administration (p=0.0031). In lung, however, there was no significant difference in cytosolic Gst activity at any of the time points (One way ANOVA = 0.5531)

Relative phase I and phase II mRNA expression in liver and lung tissue

In liver tissue, treatment with ISC-4 was found to significantly alter expression of several Gsts, Cyps, and Ugts (Figure 5A). The mean expression levels of Gsta4, Gstm1, Gstm3, and Gstp1 were increased in both the 8 h and 16 h treatment groups relative to control animals (p=0.0002, p=0.0088, p=0.0003, and p=0.0009, respectively). Expression levels reached as high as 1.6-fold higher than control animals for Gsta4, 6.9-fold higher for Gstm1, 10.8-fold higher for Gstm3, and 7.0-fold higher for Gstp1. There was no significant change in the expression of Gsta3 and Gstm2 in liver. The mean expression of Cyp2a4 and Cyp8b1 was found to be significantly increased 8 h after treatment relative to the control group (2.8-fold for Cyp2a4, p=0.0426; 4.5-fold for Cyp8b1, p=0.0026), though no increase was seen at 16 h. There was no significant change in the expression of Cyp2c29, Cyp2f2, Cyp2s1, Cyp3a11, and Cyp4b1 in either the 8 h or 16 h treatment groups. In terms of hepatic Ugt expression, Ugt1a6a was significantly higher at 8 h (5.1-fold, p=0.0045), and expression of Ugt2b5 reached as high as 2.3-fold higher than control animals at 16 h (p=0.0020). There was no significant change in the expression of Ugt1a1, Ugt1a5, Ugt2a3, or Ugt2b1. Ugt1a9 and Ugt1a10 were not expressed at detectable levels in any of the mouse liver samples examined.

Treatment with ISC-4 was also found to alter the expression levels of phase I and phase II genes in lung tissue (Figure 5B). The mean expression levels of Gstm1, Gstm3, and Gstp1 were found to be significantly higher in lung tissue of animals treated with ISC-4 (p=0.0022, p=0.0004, and p<0.0001, respectively). Expression levels reached as high as 1.5-fold higher than control animals for Gstm1, 2.5-fold higher for Gstm3, and 3.4-fold for Gstp1. No change in expression was seen for Gsta3, Gsta4, or Gstm2. Cyp expression in lung tissue was found to be significantly decreased for Cyp2f2, reaching as low as 1.8-fold lower than control animals at 16 h (p=0.0153). A small decrease in Cyp2s1 expression was also observed and approached significance at 16 h (p=0.0634). No significant change in expression was observed for Cyp4b1 or Cyp8b1. Cyp2a4, Cyp2c29, and Cyp3a11 were not expressed at detectable levels in mouse lung. Ugt1a6a and Ugt1a9 were both found to be significantly higher in lung tissue from treated animals, reaching as high as 1.9-fold for Ugt1a6a and 2.8-fold for Ugt1a9 (p=0.0132 and p=0.0150, respectively). Expression of Ugt1a1 was not found be significantly different, while Ugt1a5, Ugt1a10, Ugt2a3, Ugt2b1, and Ugt2b5 were not expressed at detectable levels.

Inhibition of DNA adduct formation in A/J mice by ISC-4

Both pob adducts resulting from the keto alcohol pathway and methyl adducts resulting from the keto acid pathway of NNK metabolism were analyzed. The levels of O^6-pob-dG in liver and lung, and levels of O^2-pob-dT in lung were decreased in mice fed with ISC-4 supplemented diet compared to control diet mice but the decreases were not significant

(Table 2). Methyl adduct analysis showed both O^6-MG and 7-MG adducts could not be detected in the lung tissues of mice fed with ISC-4 supplemental diet treated with NNK, whereas adducts were detected in mice fed control diet (Table 3). Statistics were not possible because lungs in each treatment group were pooled (n=3 or 4). Livers from three mice in each group were analyzed for methyl adducts. Significantly lower amounts of O^6-MG were seen in mice fed ISC-4 diet than mice fed control diet (p=0.033). Lower levels of 7-MG were also seen however the difference was not statistically significant (p=0.41).

Discussion

Here we report for the first time the novel compound ISC-4 when administered orally to mice results in elevated selenium levels in serum and tissue in a dose and time dependent manner as measured by atomic absorption. The highest tissue levels of selenium were obtained in serum where selenium reached a maximum at about 4 h, however it is unclear how much ISC-4 is free or bound in the serum. After a single dose of 1.25 μmol, selenium levels peaked in liver between 4–8 h and in lung at 8 h. Selenium levels begin to taper off at about 24 h for all tissues tested and may be at subclinical concentrations in its active form by this time point as suggested by the recovery of microsomal Cyp activity. Interestingly, levels of selenium do not return to control (0 h) values in serum or liver even after 72 h suggesting that ISC-4 has a long half life, remains bound to protein, or possibly that after ISC-4 is metabolized, selenium is recycled in cells as selenocysteine. The inhibition of microsomal enzyme activity as early as 0.5 h after oral dosing suggests that ISC-4 is acting directly with protein to inhibit activity. This was confirmed by direct incubation of drug with mouse liver microsomes. We predict that the reactive isoselenocyanate group of ISC-4 is most likely reacting with protein thiols, thereby inhibiting enzyme activity. The isoselenocyanate functional group has been found by our lab to be reactive to sulfhydryl (-SH) groups of thiols and therefore may bind nonspecifically to protein cysteine sulfhydryl groups (unpublished results). Our results show ISC-4 was able to inhibit microsomal metabolism using concentrations as low as 25 nM, as evidenced by the reduction in bioactivation of NNK. Similar results were also observed for Ugt enzyme activity (data not shown) with inhibition starting at about 500 nM. In the lung, the greatest inhibition of oxidative metabolites was at 8 h, when selenium levels measure the highest. The initial sharp decrease in Cyp450 activity in the liver correlated well with the time course of selenium levels in the liver. Interestingly, the peak ISC-4 level in liver (4–8 h) was not the same as the time point when NNK metabolism was the lowest in the liver (2 h) suggesting that ISC-4 might be metabolized or degraded as an inactive selenium compound and then detoxified out of the liver which would explain why selenium levels keep rising but inhibition of microsomes decreases. In both liver and lung, metabolite levels begin to increase after 8 h but then decrease again after 16 h, suggesting ISC-4 may be having both a direct effect on these enzymes as well as an indirect effect through a transcriptional mechanism.

For both the Gst and Ugt activity assays, a delayed increase in activity was found after 8 h, which we hypothesized to be driven by an increase in gene expression. This is supported by the fact that ITCs are known to be detoxified by GST enzymes in humans and are able to induce them via a transcriptional mechanism involving the antioxidant response element and the transcription factor Nrf2 (47–49). Further studies are needed to determine if ISC-4 is also able to induce the Nrf2 pathway, but the expression results suggest it does induce expression of several cytoprotective Gst genes, which are under transcriptional control of Nrf2. The same Gsts induced in liver tissue were also found to be upregulated in lung tissue. The only exception was Gsta4, which was only modestly increased in the liver and showed no change in the lung. The increases in expression seen in lung tissue were smaller in magnitude than the increases seen in the liver, which correlate to the higher levels of selenium reached in the liver compared to the lung.

Delayed increases in activity of Ugt enzymes in mouse liver may have cytoprotective effects as well. Eight hours after treatment, there was a transient increase in the levels of two Phase I genes, Cyp2a4 and Cyp8b1, but by 16 h this effect had disappeared. Since Phase I expression levels returned to normal rather quickly while Phase II genes remained upregulated, the potential negative effects of increased Cyp activity may be overcome by the sustained increase in Phase II genes. To explore Ugt activity the major detoxification metabolite of NNK, NNAL, was used. In humans, UGTs 1A4, 1A9, 2B7, 2B10, and 2B17 isoforms (see Table 3 for orthologs) all exhibit activity against NNAL. Glucuronidation of NNAL was significantly increased after 8 h, which may be explained by the transcriptional upregulation of the UGT2B10 ortholog Ugt2b34. Lung microsomes typically show poor activity against NNAL, which may be explained by the lack of 2B isoforms expressed in the lung, specifically 2B10. In A/J mouse lung no detectable expression of 2B orthologs tested in this study were found. We therefore used a second substrate, 4-MU, to explore glucuronidation activity in both liver and lung which is ubiquitously conjugated by most UGTs. Interestingly, in liver microsomes, no change in glucuronidation activity was seen over time against 4-MU. This data suggests that ISC-4 may be having an effect only on certain Ugt isoforms, in this case the 2b family, a possibility that needs to be further investigated. For lung microsomes, activity against 4-MU was significantly increased at 24 h, which may be explained by the upregulation seen in Ugt1a9, which is not expressed in liver. Some Ugts, such as Ugt1a6a were significantly upregulated in both tissues, while Ugt1a1 was unchanged in both tissues, which suggests that ISC-4-induced changes in Ugt expression could occur by the same regulatory mechanism in these two tissues for these particular enzymes.

The modulation of Phase I and II enzymes by ISC-4 led us to develop a bioassay to determine if ISC-4 could inhibit DNA adduct formation in vivo. Our results demonstrated that O^6-MG adduct formation was significantly inhibited in the liver of A/J mice and in lung these adducts were not detectable in mice treated with NNK and fed with the ISC-4 supplemented diet. The inhibition of methyl adducts formation in both liver and lung is most likely due to the inhibition of Cyp enzyme activity and possibly to the upregulation of individual Ugts responsible for NNAL detoxification.

In conclusion, ISC-4 given to A/J mice appears to be bioavailable, causes increased selenium levels in tissue and serum, and results in modified activity and expression of both Phase I and II enzymes critical for bioactivation and detoxification of many carcinogens. ISC-4 fed to mice in the diet resulted in decreased DNA adducts from NNK critical for carcinogenesis. Taken together, ISC-4 may be a suitable chemopreventive agent due to its anti-initiation effects of inhibiting carcinogen metabolism and increasing detoxification.

Acknowledgments

The authors thank the Macromolecular Core Facility and the Genomics Core of the Pennsylvania State University, College of Medicine, for recording mass spectra and bioanalysis of RNA samples, respectively.

Grant Support: This study was supported by the National Institutes of Health National Cancer Institute Grant R03-CA143999 (A. K. S.), the National Institutes of Health National Institute of Dental and Craniofacial Research Grant R01-DE13158 (P.L.), and the Pennsylvania Department of Health's Health Research Formula Funding Program Grants 4100038714 (P.L.) and 4100038715 (P.L.)

References

1. Jemal A, Siegel R, Xu J, Ward E. Cancer statistics, 2010. CA Cancer J Clin. 60:277–300. [PubMed: 20610543]
2. Novello, AC. Smoking and Tobacco Control Monograph No. 2. General, S., editor. 2008. p. ix-xv.

3. Talalay P, Fahey JW. Phytochemicals from cruciferous plants protect against cancer by modulating carcinogen metabolism. J Nutr. 2001; 131:3027S–3033S. [PubMed: 11694642]
4. Verhoeven DT, Goldbohm RA, van Poppel G, Verhagen H, van den Brandt PA. Epidemiological studies on brassica vegetables and cancer risk. Cancer Epidemiol Biomarkers Prev. 1996; 5:733–748. [PubMed: 8877066]
5. Higdon JV, Delage B, Williams DE, Dashwood RH. Cruciferous vegetables and human cancer risk: epidemiologic evidence and mechanistic basis. Pharmacol Res. 2007; 55:224–236. [PubMed: 17317210]
6. Fahey JW, Zalcmann AT, Talalay P. The chemical diversity and distribution of glucosinolates and isothiocyanates among plants. Phytochemistry. 2001; 56:5–51. [PubMed: 11198818]
7. Drewnowski A, Gomez-Carneros C. Bitter taste, phytonutrients, and the consumer: a review. Am J Clin Nutr. 2000; 72:1424–1435. [PubMed: 11101467]
8. Cinciripini PM, Hecht SS, Henningfield JE, Manley MW, Kramer BS. Tobacco addiction: implications for treatment and cancer prevention. J Natl Cancer Inst. 1997; 89:1852–1867. [PubMed: 9414173]
9. Chung FL, Jiao D, Conaway CC, Smith TJ, Yang CS, Yu MC. Chemopreventive potential of thiol conjugates of isothiocyanates for lung cancer and a urinary biomarker of dietary isothiocyanates. J Cell Biochem Suppl. 1997; 27:76–85. [PubMed: 9591196]
10. Stoner GD, Adams C, Kresty LA, Amin SG, Desai D, Hecht SS, Murphy SE, Morse MA. Inhibition of N'-nitrosonornicotine-induced esophageal tumorigenesis by 3-phenylpropyl isothiocyanate. Carcinogenesis. 1998; 19:2139–2143. [PubMed: 9886569]
11. Traka M, Mithen R. Glucosinolates, isothiocyanates and human health. Phytochem Rev. 2009; 8:269–282.
12. Chung KY, Saltz LB. Adjuvant therapy of colon cancer: current status and future directions. Cancer J. 2007; 13:192–197. [PubMed: 17620769]
13. Yu R, Mandlekar S, Harvey KJ, Ucker DS, Kong AN. Chemopreventive isothiocyanates induce apoptosis and caspase-3-like protease activity. Cancer Res. 1998; 58:402–408. [PubMed: 9458080]
14. Zhang Y, Talalay P. Anticarcinogenic activities of organic isothiocyanates: chemistry and mechanisms. Cancer Res. 1994; 54:1976s–1981s. [PubMed: 8137323]
15. Maheo K, Morel F, Langouet S, Kramer H, Le Ferrec E, Ketterer B, Guillouzo A. Inhibition of cytochromes P-450 and induction of glutathione S-transferases by sulforaphane in primary human and rat hepatocytes. Cancer Res. 1997; 57:3649–3652. [PubMed: 9288764]
16. Kassahun K, Davis M, Hu P, Martin B, Baillie T. Biotransformation of the naturally occurring isothiocyanate sulforaphane in the rat: identification of phase I metabolites and glutathione conjugates. Chem Res Toxicol. 1997; 10:1228–1233. [PubMed: 9403174]
17. Morse MA, Eklind KI, Hecht SS, Jordan KG, Choi CI, Desai DH, Amin SG, Chung FL. Structure-activity relationships for inhibition of 4-(methylnitrosamino)-1-(3-pyridyl)-1-butanone lung tumorigenesis by arylalkyl isothiocyanates in A/J mice. Cancer Res. 1991; 51:1846–1850. [PubMed: 2004368]
18. Jiao D, Eklind KI, Choi CI, Desai DH, Amin SG, Chung FL. Structure-activity relationships of isothiocyanates as mechanism-based inhibitors of 4-(methylnitrosamino)-1-(3-pyridyl)-1-butanone-induced lung tumorigenesis in A/J mice. Cancer Res. 1994; 54:4327–4333. [PubMed: 8044780]
19. Hecht SS. Biochemistry, biology, and carcinogenicity of tobacco-specific N-nitrosamines. Chem Res Toxicol. 1998; 11:559–603. [PubMed: 9625726]
20. Staretz ME, Foiles PG, Miglietta LM, Hecht SS. Evidence for an important role of DNA pyridyloxobutylation in rat lung carcinogenesis by 4-(methylnitrosamino)-1-(3-pyridyl)-1-butanone: effects of dose and phenethyl isothiocyanate. Cancer Res. 1997; 57:259–266. [PubMed: 9000565]
21. Sticha KR, Kenney PM, Boysen G, Liang H, Su X, Wang M, Upadhyaya P, Hecht SS. Effects of benzyl isothiocyanate and phenethyl isothiocyanate on DNA adduct formation by a mixture of benzo[a]pyrene and 4-(methylnitrosamino)-1-(3-pyridyl)-1-butanone in A/J mouse lung. Carcinogenesis. 2002; 23:1433–1439. [PubMed: 12189184]

22. Boysen G, Kenney PM, Upadhyaya P, Wang M, Hecht SS. Effects of benzyl isothiocyanate and 2-phenethyl isothiocyanate on benzo[a]pyrene and 4-(methylnitrosamino)-1-(3-pyridyl)-1-butanone metabolism in F-344 rats. Carcinogenesis. 2003; 24:517–525. [PubMed: 12663513]
23. Foiles PG, Akerkar SA, Carmella SG, Kagan M, Stoner GD, Resau JH, Hecht SS. Mass spectrometric analysis of tobacco-specific nitrosamine-DNA adducts in smokers and nonsmokers. Chem Res Toxicol. 1991; 4:364–368. [PubMed: 1912321]
24. Schlobe D, Holze D, Richter E, Tricker AR. Determination of tobacco-specific nitrosamine hemoglobin and lung DNA adducts. Proc. Am. Assoc. Cancer Res. 2002; 43:346.
25. Peterson LA, Hecht SS. O6-methylguanine is a critical determinant of 4-(methylnitrosamino)-1-(3-pyridyl)-1-butanone tumorigenesis in A/J mouse lung. Cancer Res. 1991; 51:5557–5564. [PubMed: 1913675]
26. Peterson LA, Mathew R, SE BPM, Trushin N, Hecht SS. In vivo and in vitro persistence of pyridyloxobutyl DNA adducts from 4-(methylnitrosamino)-1-(3-pyridyl)-1-butanone. Carcinogenesis. 1991; 12:2069–2072. [PubMed: 1934291]
27. Sharma AK, Sharma A, Desai D, Madhunapantula SV, Huh SJ, Robertson GP, Amin S. Synthesis and anticancer activity comparison of phenylalkyl isoselenocyanates with corresponding naturally occurring and synthetic isothiocyanates. J Med Chem. 2008; 51:7820–7826. [PubMed: 19053750]
28. Reddy BS, Wynn TT, el-Bayoumy K, Upadhyaya P, Fiala E, Rao CV. Evaluation of organoselenium compounds for potential chemopreventive properties in colon cancer. Anticancer Res. 1996; 16:1123–1127. [PubMed: 8702223]
29. Clark LC, Combs GF Jr, Turnbull BW, Slate EH, Chalker DK, Chow J, Davis LS, Glover RA, Graham GF, Gross EG, Krongrad A, Lesher JL Jr, Park HK, Sanders BB Jr, Smith CL, Taylor JR. Effects of selenium supplementation for cancer prevention in patients with carcinoma of the skin. A randomized controlled trial. Nutritional Prevention of Cancer Study Group. Jama. 1996; 276:1957–1963. [PubMed: 8971064]
30. Combs GF Jr, G W. Chemopreventive Agents: Selenium. Pharmacol Ther. 1998; 79:179–192. [PubMed: 9776375]
31. Jacobs ET, Jiang R, Alberts DS, Greenberg ER, Gunter EW, Karagas MR, Lanza E, Ratnasinghe L, Reid ME, Schatzkin A, Smith-Warner SA, Wallace K, Martinez ME. Selenium and colorectal adenoma: results of a pooled analysis. J Natl Cancer Inst. 2004; 96:1669–1675. [PubMed: 15547179]
32. Ip C, Ganther HE. Comparison of selenium and sulfur analogs in cancer prevention. Carcinogenesis. 1992; 13:1167–1170. [PubMed: 1638682]
33. Sharma A, Sharma AK, Madhunapantula SV, Desai D, Huh SJ, Mosca P, Amin S, Robertson GP. Targeting Akt3 signaling in malignant melanoma using isoselenocyanates. Clin Cancer Res. 2009; 15:1674–1685. [PubMed: 19208796]
34. Witschi H. A/J mouse as a model for lung tumorigenesis caused by tobacco smoke: strengths and weaknesses. Exp Lung Res. 2005; 31:3–18. [PubMed: 15765916]
35. Guengerich, FP. Analysis and characterization of enzymes. In: Hayes, AW., editor. Principles and Methods of Toxicology. New York: Raven Press; 1994. p. 1259-1313.
36. Bustin SA. Absolute quantification of mRNA using real-time reverse transcription polymerase chain reaction assays. J Mol Endocrinol. 2000; 25:169–193. [PubMed: 11013345]
37. Derveaux S, Vandesompele J, Hellemans J. How to do successful gene expression analysis using real-time PCR. Methods. 50:227–230. [PubMed: 19969088]
38. Hellemans J, Preobrazhenska O, Willaert A, Debeer P, Verdonk PC, Costa T, Janssens K, Menten B, Van Roy N, Vermeulen SJ, Savarirayan R, Van Hul W, Vanhoenacker F, Huylebroeck D, De Paepe A, Naeyaert JM, Vandesompele J, Speleman F, Verschueren K, Coucke PJ, Mortier GR. Loss-of-function mutations in LEMD3 result in osteopoikilosis, Buschke-Ollendorff syndrome and melorheostosis. Nat Genet. 2004; 36:1213–1218. [PubMed: 15489854]
39. Suzuki T, Higgins PJ, Crawford DR. Control selection for RNA quantitation. Biotechniques. 2000; 29:332–337. [PubMed: 10948434]
40. Thellin O, Zorzi W, Lakaye B, De Borman B, Coumans B, Hennen G, Grisar T, Igout A, Heinen E. Housekeeping genes as internal standards: use and limits. J Biotechnol. 1999; 75:291–295. [PubMed: 10617337]

41. Vandesompele J, De Preter K, Pattyn F, Poppe B, Van Roy N, De Paepe A, Speleman F. Accurate normalization of real-time quantitative RT-PCR data by geometric averaging of multiple internal control genes. Genome Biol. 2002; 3 RESEARCH0034.

42. Warrington JA, Nair A, Mahadevappa M, Tsyganskaya M. Comparison of human adult and fetal expression and identification of 535 housekeeping/maintenance genes. Physiol Genomics. 2000; 2:143–147. [PubMed: 11015593]

43. Chen G, Dellinger RW, Sun D, Spratt TE, Lazarus P. Glucuronidation of tobacco-specific nitrosamines by UGT2B10. Drug Metab Dispos. 2008; 36:824–830. [PubMed: 18238858]

44. Ren Q, Murphy SE, Zheng Z, Lazarus P. O-Glucuronidation of the lung carcinogen 4-(methylnitrosamino)-1- (3-pyridyl)-1-butanol (NNAL) by human UDP-glucuronosyltransferases 2B7 and 1A9. Drug Metab Dispos. 2000; 28:1352–1360. [PubMed: 11038164]

45. Stone AN, Mackenzie PI, Galetin A, Houston JB, Miners JO. Isoform selectivity and kinetics of morphine 3- and 6-glucuronidation by human udp-glucuronosyltransferases: evidence for atypical glucuronidation kinetics by UGT2B7. Drug Metab Dispos. 2003; 31:1086–1089. [PubMed: 12920162]

46. Eklund BI, Edalat M, Stenberg G, Mannervik B. Screening for recombinant glutathione transferases active with monochlorobimane. Anal Biochem. 2002; 309:102–108. [PubMed: 12381368]

47. Conaway CC, Yang YM, Chung FL. Isothiocyanates as cancer chemopreventive agents: their biological activities and metabolism in rodents and humans. Curr Drug Metab. 2002; 3:233–255. [PubMed: 12083319]

48. Owuor ED, Kong AN. Antioxidants and oxidants regulated signal transduction pathways. Biochem Pharmacol. 2002; 64:765–770. [PubMed: 12213568]

49. Hong F, Freeman ML, Liebler DC. Identification of sensor cysteines in human Keap1 modified by the cancer chemopreventive agent sulforaphane. Chem Res Toxicol. 2005; 18:1917–1926. [PubMed: 16359182]

50. Blake JA, Bult CJ, Kadin JA, Richardson JE, Eppig JT. The Mouse Genome Database (MGD): premier model organism resource for mammalian genomics and genetics. Nucleic Acids Res. 39:D842–D848. [PubMed: 21051359]

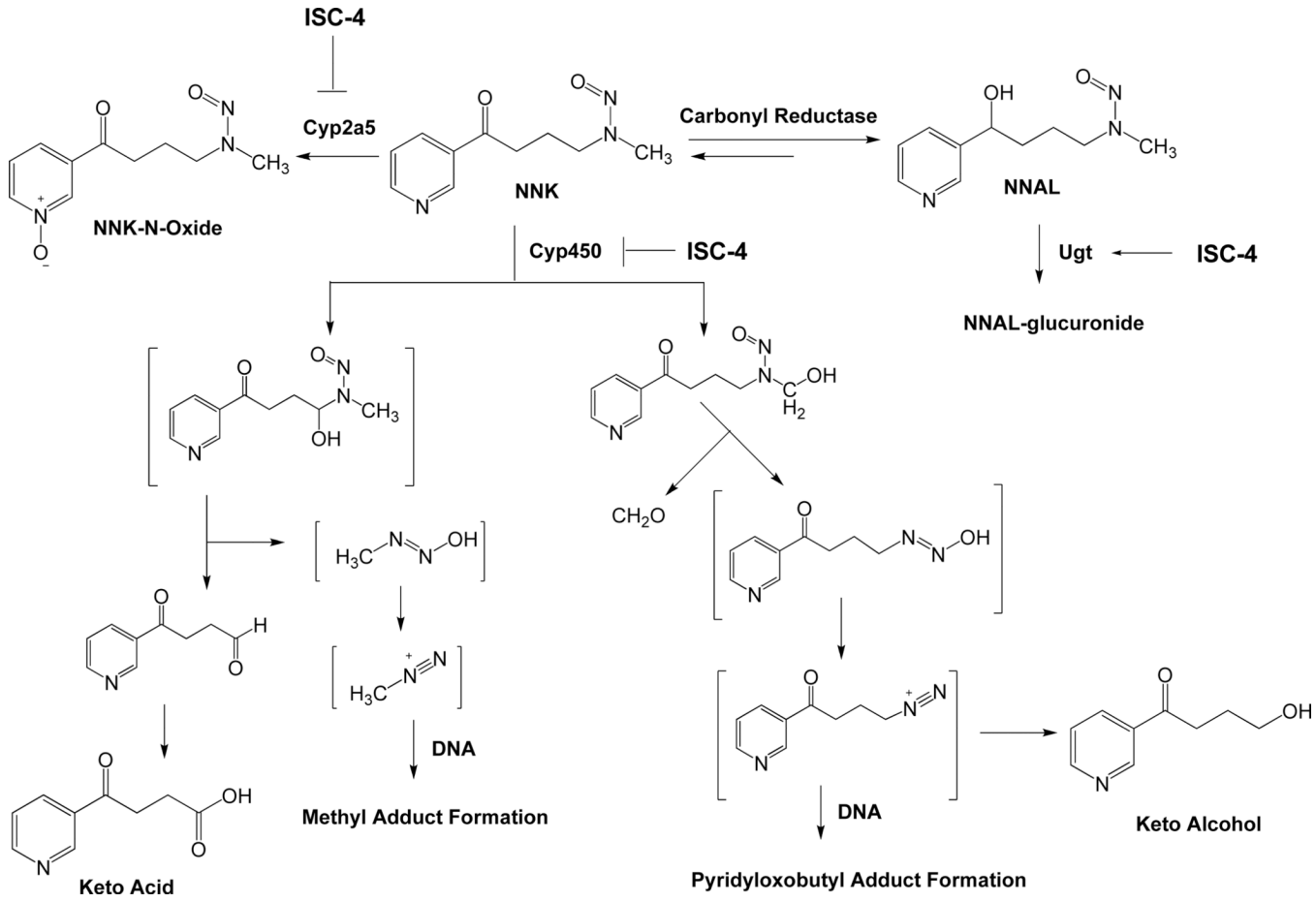

Figure 1.
Bioactivation and detoxification pathways of NNK.

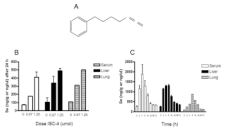

Figure 2.
Phenylbutyl isoselenocyanate (ISC-4) and its intragastric (IG) administration in A/J mice. A, structure of (ISC-4). B, selenium levels in serum, liver, and lung tissue of A/J mice treated with corn oil (vehicle), 0.675 μmol, or 1.25 μmol ISC-4 after 24 h. C, selenium levels in A/J mice from serum, liver, and lung tissue taken at 2, 4, 8, 16, 24, 36, and 72 h after 1.25 μmol dose of ISC-4.

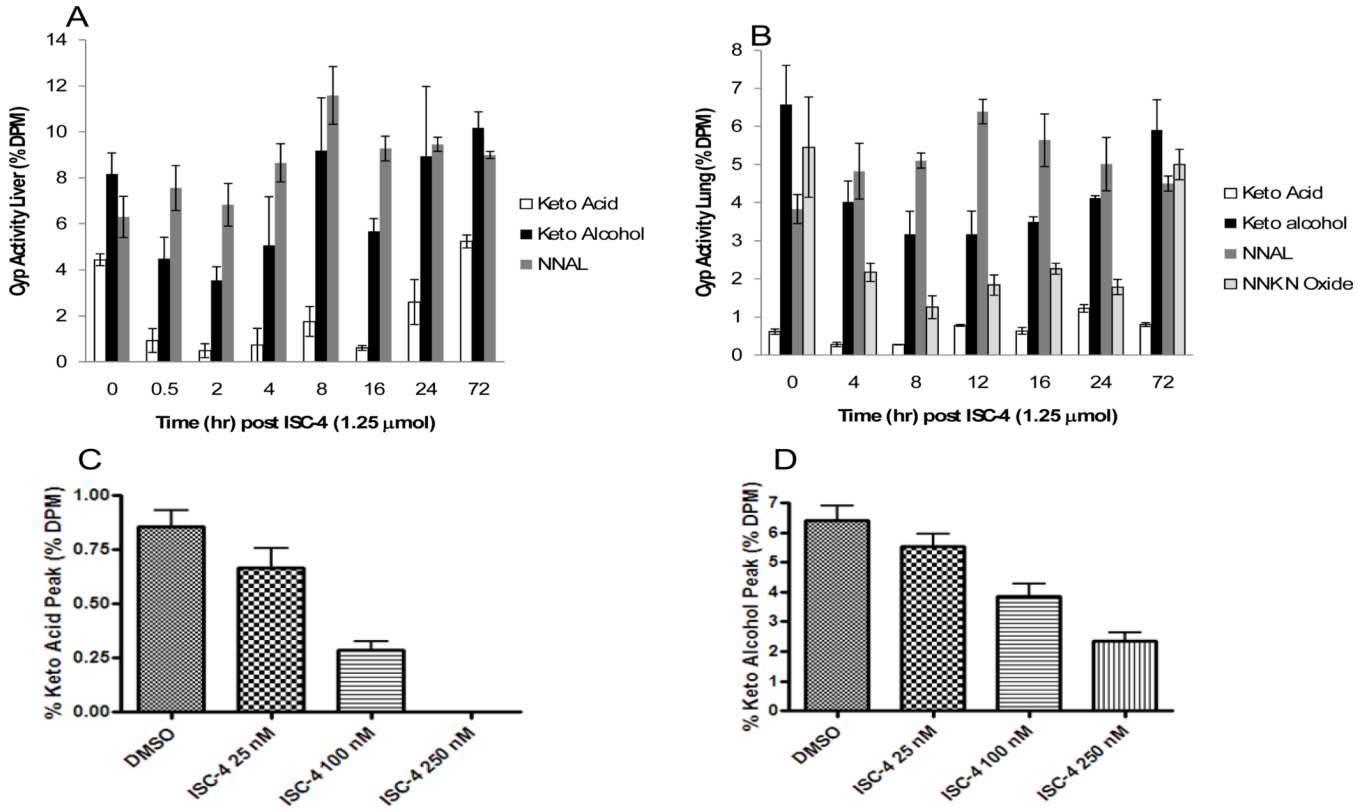

Figure 3.

Effects of ISC-4 on Phase I metabolism of NNK by A/J mice microsomes. A, metabolism of ^{3}H[NNK] by liver microsomes at time points 0, 0.5, 2, 4, 8, 16, 24, and 72 h post ISC-4 administration (1.25 μmol in 100 μl corn oil IG). B, metabolism of ^{3}H[NNK] by lung microsomes at time points 0, 4, 8, 12, 16, 24, and 72 h post ISC-4 administration (1.25 μmol in 100 μl corn oil IG). C, effect of in vitro incubation of ISC-4 on control liver microsome metabolism of NNK to keto acid. D, effect of in vitro incubation of ISC-4 on control liver microsome metabolism of NNK to keto alcohol.

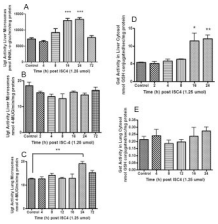

Figure 4.

Effects of ISC-4 on Phase II metabolism in A/J mice. Mice were treated with 1.25 μmol ISC-4 dissolved in 100 μl corn oil IG. A, glucuronidation of NNAL by liver microsomes at 0, 4, 8, 16, 24, and 72 h after administration of ISC-4. B, glucuronidation of 4-MU by liver microsomes at 0, 2, 4, 8, 16, 24, and 72 h after administration of ISC-4. C, glucuronidation of 4-MU by lung microsomes at 0, 4, 8, 12, 16, 24, and 72 h after administration of ISC-4. D, glutathione conjugation of MCB by liver cytosol of A/J mice at 0, 2, 4, 8, 16, and 24 h after administration of ISC-4. E, glutathione conjugation of MCB by lung cytosol of A/J mice at 0, 4, 8, 12, 16, and 24 h after administration of ISC-4.

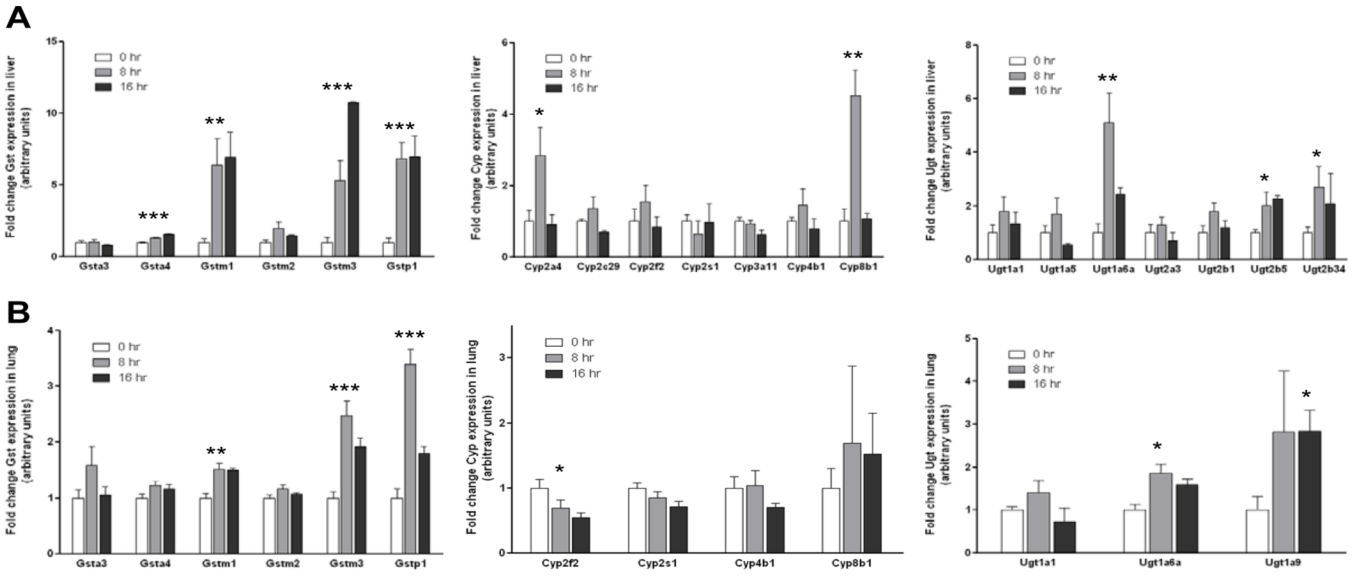

Figure 5.

Effects of ISC-4 on Phase I and Phase II gene expression. Mice were treated with 1.25 μmol ISC-4 dissolved in 100 μl corn oil IG. A, fold change of liver Gst, Cyp, and Ugt mRNA isoforms in A/J mice at 8 and 16 h after administration of ISC-4 compared to corn oil control. B, fold change of lung Gst, Cyp, and Ugt mRNA isoforms in A/J mice at 8 and 16 h after administration of ISC-4 compared to corn oil control.

Table 1

Genotyped Mouse Phase I and Phase II Human Orthologs[50]

Phase I - Cyp		Phase II - Ugt		Phase II - Gst	
Human	**Murine**	**Human**	**Murine**	**Human**	**Murine**
CYP2A6‡†, CYP2A7	Cyp2a4,Cyp2a5	UGT1A4*	Ugt1a5	GSTA3	Gsta3
CYP2F1‡	Cyp2f2	UGT1A1	Ugt1a1	GSTA4	Gsta4
CYP2S1	Cyp2s1	UGT1A6	Ugt1a6a	GSTP1	Gstp1
CYP4B1	Cyp4b1	UGT2B4	Ugt2b1	GSTM2	Gstm2
NF (2D6 superfamily)†	Cyp2c29	NF	Ugt2b5	GSTM3	Gstm3
NF (3A5 superfamily)‡	Cyp3a11	UGT2B10*	Ugt2b34	GSTM1/M5	Gstm1
CYP8B1	Cyp8b1	UGT2B15	Ugt2b35		
		UGT2A3	Ugt2a3		
		UGT1A9*	Ugt1a9		
		NF	Ugt1a10		
		UGT2B15	Ugt2b36		

NF - no ortholog found

‡Isoforms found to bioactivate NNK to keto alcohol

†Isoforms found to bioactivate NNK to keto acid

*Isoforms found to glucuronidate NNAL

Table 2

Pyridyloxobutyl (pob) DNA adduct formation (fmol adduct/nmol G/T)

Groups	Liver		Lung	
	O^2-pob dT	O^6-pob dG	O^2-pob dT	O^6-pob dG
Untreated /Control Diet	n.d.	n.d.	n.d.	n.d.
NNK Treated /Control Diet	16.21 +/− 4.75	2.29 +/− 0.87	2.98 +/− 1.24	0.20 +/− 0.35
NNK Treated/ ISC-4 Diet	22.02 +/− 5.62[n.s]	1.78 +/− 0.90[n.s.]	1.95 +/− 0.84[n.s]	n.d.

n.s. - not significant p = 0.35, 0.57, and 0.33

n.d. - not detected

Table 3

Methyl DNA adduct formation (pmol adduct/nmol G)

Groups	Liver		Lung (pool)	
	O^6-MG	7-MG	O^6-MG	7-MG
Untreated /Control Diet	n.d.	0.29 +/− 0.04	n.d	0.56
NNK Treated /Control Diet	5.18 +/− 1.33	3.28 +/− 1.39	11.22	13.27
NNK Treated/ ISC-4 Diet	1.75 +/− 1.31†	2.54 +/− 0.08	n.d.	n.d.

† p = 0.0031 vs. NNK treated/Control Diet

n.d. - not detected